Interplay between optical nonlinearity and localization in a finite disordered Fibonacci chain

Tony Huang*
8217 R.C. Gorman Avenue Northeast, Albuquerque, New Mexico 87122, USA

Danhong Huang†
Air Force Research Laboratory (AFRL/VSSS), Kirtland Air Force Base, New Mexico 87117, USA
(Received 4 December 2006; revised manuscript received 19 March 2007; published 5 July 2007)

Both the average transmission coefficients and dimensionless optical resistances of a nonlinear disordered Fibonacci chain are calculated as functions of the photon flux of an incident light field with various types of chains of scatters, numbers of embedded nonlinear-optical scatterers, and energies of incident photons. If the incident optical field is very weak, the nonlinear-optical scattering in the chain becomes negligible and the chain behaves just like a transparent dielectric slab. As for the interplay between the optical nonlinearity and localization effect in the finite disordered Fibonacci chain, it is found that the localization effect introduced in the disordered Fibonacci chain exhibits a reduction in the transmission only when the incident optical field is strong. The localization effect, which increases with the number of scatterers in the chain, is found to yield an enhanced optical nonlinearity of the system. The localization effect on the incident optical wave in the chain can be accelerated by an intense light illumination in the presence of a large number of nonlinear-optical scatterers. When energetic photons fly through the chain, they tend to ignore most of the deeply embedded optical scatterers. When the number of scatterers in the system is $F_{16}=1597$, a complete localization in the chain is reached for an incident field amplitude as low as 50 kV/cm.

DOI: 10.1103/PhysRevB.76.024201 PACS number(s): 72.15.Rn, 42.65.−k, 42.70.Qs, 42.70.Nq

I. INTRODUCTION

Photodetector and vision protection against high-power laser damage[1–3] are very desirable in many optoelectronic applications. For the exposure of optoelectronic devices to high-power radiation, it is important to develop a protection scheme which makes use of the intensity dependence of transmittance to block harmful radiation over a broad wavelength range. At the same time, it should also be transparent to low-power radiation in visible wavelengths for human vision purposes. Current protection schemes using the photochromic effect or two-photon absorption usually reject only a limited number of laser frequencies and have no dependence of transmission on the incident laser power. Nonlinear one-dimensional (1D) photonic band-gap structures (PBSs) have proven to be promising candidates for laser-damage protection.[4] Such smart devices allow high transmission for low-intensity light but block high-intensity radiation in a wide-spectral range with fast response and recovery time.

The central blocking frequency of PBS can be designed by choosing different material compositions and structures.[5–9] The classic picture of PBS is photon localization, involving interference among multiple scattered waves in a random medium. Interference among these waves in the medium confines the wave within a region the size of a localization length.[10] If the size of the material system becomes greater than the localization length, the diffusion coefficient for wave propagation becomes zero. In order to reject high-power radiation, nonlinear-optical materials with an intensity-dependent refractive index[11] can be employed. The combination of principles of PBS and nonlinear optics can create 1D nonlinear photonic band gaps, which exclude electromagnetic radiation over a band of frequencies when the light intensity is high.[4]

Recent technical advances in submicron physics have further enabled experimentalists to fabricate nearly ideal multilayer PBS using molecular-beam epitaxy growth techniques[12] or sputtering. The connection between the electrical resistance at zero temperature and the transmission coefficient, provided by the well-known Landauer formula,[13] indicates that some experimentally measurable quantities, such as electrical or optical resistance, can be adequately explained when a simple infinite 1D array of short-range electronic or optical scatterers is considered. The discovery of quasicrystals[14] has stimulated interest in exploring the physical nature of quasiperiodic (e.g., Fibonacci and Thue-Morse) sequences[15] as well as commensurate-incommensurate systems.[16] Our previous researches on quasiperiodic sequences included plasmon excitation,[17] electron localization,[18,19] neutron polarization,[20] phonon density of states,[21] optical-phonon tunneling,[22] nonlinear-optical filters,[4] defect-assisted tunneling,[23] and interaction between two nonlinear electron waves.[24] The quasiperiodicity in an infinite chain leads to a self-similar structure in the transmission as a function of the incident energy. The disordered (fully random) chain leads to Anderson localization[10] only when the chain becomes infinitely long. For a short disordered chain, there is no complete localization. However, when the chain length practically exceeds a threshold value, i.e., the localization length, the electronic or optical wave behaves very similar to that found when there is complete localization. In this case, the transmission of a long chain with disorder can be exponentially small.

The pure Fibonacci numbers, 1, 1, 2, 3, 5, 8, 13,…, defined via the recurrence $F_{n+1}=F_n+F_{n-1}$, were found to relate to the number of leaves, petals, or seed grains in plants and ancestors of a drone in nature. A straightforward stochastic modification of the pure Fibonacci sequence is to introduce both additions and subtractions. The random Fibonacci recurrence $x_{n+1}=x_n\pm x_{n-1}$ results in sequences which behave erratically for small generation index n. In the limit of n

$\rightarrow\infty$, however, exponential growth occurs with unit probability as was demonstrated by Furstenberg[25] in 1963. For the random Fibonacci recurrence where each $\pm$ sign is independent and occurs with probability 1/2, the Lyapunov exponent $\nu=0.123\,975\,58\ldots$ is found.[26] Very recently, the renormalization-group method has been generalized[29] to study the local electronic properties of large disordered Fibonacci chains in which different generations of pure Fibonacci chains and inverted Fibonacci chains (see the definition in the next section) are randomly mixed (concatenation rule).[27] The Lyapunov exponents for the weak and strong disordered cases can also be calculated numerically.[28]

In this paper, we compute the average transmission coefficients and dimensionless nonlinear-optical resistances for an incident light wave packet as functions of the incident photon flux for disordered and pure Fibonacci chains, different generations of Fibonacci sequences, as well as different photon energies. We demonstrate that localization effect in a disordered Fibonacci chain can play a role if the light illumination is intense. We further find that the optical nonlinearity in the disordered Fibonacci chain can be enforced by the localization effect increasing with the number of embedded nonlinear-optical scatterers in the system. An intense incident light field can speed up the localization effect on an optical wave if there are enough optical scatterers present in the chain. The higher the photon energy is, the less the effective number of scatterers will be felt by photons flying through the chain. Interesting physics behind the interplay between the optical nonlinearity and localization effect in a finite disordered Fibonacci chain is elucidated.

The organization of the paper is as follows. In Sec. II, we introduce our model and theory for the calculations of average transmission coefficient and nonlinear-optical resistance (see its definition in the next section) with layered nonlinear-optical scatterers embedded in a disordered Fibonacci chain. Numerical results are displayed and explained in Sec. III for the average transmission coefficient and optical resistances as functions of the field amplitude of incident light. The paper is briefly concluded in Sec. IV.

II. MODEL AND THEORY

Let us start by considering a plane-polarized electromagnetic wave with frequency ω, which propagates parallel to the z direction perpendicular to the interfaces of a multilayer structure shown in Fig. 1. The multilayer structure in this figure is composed of a nondissipative (no optical absorption) dielectric slab embedded with many planar nonlinear-optical scatterers. For simplicity, we assume a matched refractive index to dielectric materials surrounding the multilayer structure. The form of plane-polarized and single-color optical field can be simply written as $E(z,t)=E(z)\exp(-i\omega t)$ within the multilayer structure. The z-dependent field amplitude $E(z)$ satisfies the following 1D Maxwell wave equation:

$$\frac{d^2E(z)}{dz^2}+\frac{\omega^2}{c^2}n_r^2(z)E(z)=0, \tag{1}$$

where the z-dependent refractive-index function $n_r(z)$, including layered nonlinear-optical scatterers, is

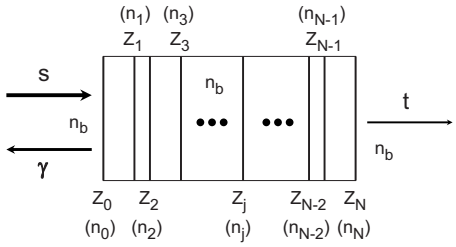

FIG. 1. Illustration of a finite nonlinear disordered Fibonacci chain embedded with optical scatterers at $z_0,z_1,\ldots,z_j,\ldots,z_{N-1},z_N$, where the positions of optical scatterers $\{z_1,z_2,\ldots,z_{N-1},z_N\}$ form a so-called disordered Fibonacci sequence (see the text) with the position of the first optical scatterer fixed at $z=z_0=0$. The linear refractive index of the chain is n_b, and the nonlinear refractive index for the jth optical scatterer at $z=z_j$ is n_j. The space outside the sample ($z<z_0$ and $z>z_N$) is filled by a dielectric material with a matched refractive index n_b. The light is incident from the left of the sample ($z<z_0$) and is transmitted to the right of the sample ($z>z_N$). The field amplitudes of the incident, reflected, and transmitted optical waves in this figure are denoted as s, γ, and t, respectively.

$$n_r(z)=n_b+\sum_{j=0}^{N}n_j\delta(z-z_j). \tag{2}$$

Here, z_j is the position of the jth planar optical scatterer, $(N+1)$ is the total number of scatterers, n_b is the linear refractive index of the dielectric slab, and the nonlinear refractive index n_j of the jth optical scatterer is assumed to be[4]

$$n_j=(-1)^{j+1}\beta_K|E(z_j)|^2,\quad 0\leqslant j\leqslant N, \tag{3}$$

where β_K is the Kerr nonlinear coefficient and $|E(z_j)|$ is the field amplitude at the jth optical scatterer.

If the positions of the optical scatterers for the $(n-1)$th and nth generations of a pure Fibonacci chain are denoted by $\{x_1,x_2,\ldots,x_{F_{n-1}}\}$ and $\{y_1,y_2,\ldots,y_{F_n}\}$, respectively, we can obtain the positions of the optical scatterers for the $(n+1)$th generation at $\{z_1,z_2,\ldots,z_{F_{n+1}}\}$ through the relation[19]

$$z_j=\begin{cases}y_j & \text{for } j=1,\ldots,F_n\\ y_{F_n}+x_{j-F_n} & \text{for } j=(F_n+1),\ldots,F_{n+1},\end{cases} \tag{4}$$

with $z_1=b$ and $z_2=b+a$, where a and b are two arbitrary real numbers, and F_n is the nth number in a Fibonacci sequence $\{F_1,F_2,\ldots,F_{n-1},F_n,F_{n+1},\ldots\}$. The numbers in the Fibonacci sequence are obtained through the recurrence $F_{n+1}=F_n+F_{n-1}$ starting from $F_1=1$ and $F_2=2$.

In this work, we further define an inverted Fibonacci chain. For this situation, instead of using Eq. (4) we define the positions of optical scatterers for the $(n+1)$th generation through a concatenation rule[19,29]

$$z_j=\begin{cases}x_j & \text{for } j=1,\ldots,F_{n-1}\\ x_{F_{n-1}}+y_{j-F_{n-1}} & \text{for } j=(F_{n-1}+1),\ldots,F_{n+1}.\end{cases} \tag{5}$$

The so-called disordered Fibonacci chain is the random mix of the pure and inverted Fibonacci chains in Eqs. (4) and (5). We introduce a random variable η which is uniformly dis-

tributed within the interval $0<\eta<1$. For any given real number $0\leqslant p\leqslant 1$, we define a disordered Fibonacci chain as follows: the disordered Fibonacci chain becomes the pure Fibonacci chain if $\eta<p$, while the disordered Fibonacci chain becomes the inverted Fibonacci chain if $\eta\geqslant p$. Therefore, the disordered Fibonacci chain simply reduces to the pure Fibonacci chain when $p=1$. On the other hand, the disordered Fibonacci chain reduces to the inverted Fibonacci chain when $p=0$. When $p=1/2$, however, there is an equal probability for the disordered Fibonacci chain to become either the pure or the inverted Fibonacci chain. For $p=1/2$, the randomness of the system reaches a maximum.

As shown in Fig. 1, we assume that the multilayer structure occupying the region $z_0\leqslant z\leqslant z_N$ (with a fixed $z_0=0$) is under a light illumination from the left, where $z<z_0$ is filled by a dielectric material with a matched refractive index n_b, and then transmitted to the right, where $z>z_N$ is also filled by the index-matched dielectric material. Here, the number set $\{z_1,z_2,\ldots,z_{N-1},z_N\}$ is assumed to be a disordered Fibonacci sequence, with $N=F_n$ being the number of optical scatterers for the nth generation disordered Fibonacci chain (excluding the first optical scatterer fixed at $z=z_0=0$). For this case, the solution to Eq. (1) can be formally written as[4,30]

$$E(z)=\begin{cases} se^{iqz}+\gamma e^{-iqz} & \text{if } z<z_0=0 \\ f_j e^{iq(z-z_j)}+b_j e^{-iq(z-z_j)} & \text{if } z_{j-1}<z<z_j \\ te^{iqz} & \text{if } z>z_N, \end{cases} \tag{6}$$

where $j=1,2,\ldots,N$, and the wave number along the z direction is $q\equiv q_0 n_b=2\pi n_b/\lambda_0$, with $\lambda_0=2\pi c/\omega$ denoting the wavelength and c the speed of light in vacuum. The quantities f_j and b_j are known as the coefficients for the forward and backward optical waves[19] between the $(j-1)$th and the jth optical scatterers with $1\leqslant j\leqslant N$ and are determined by the boundary conditions at different scatterers. In addition, s, γ, and t in Eq. (6) are the field amplitudes of the incident, reflected, and transmitted optical waves, respectively.

By assuming a moderate incident optical field, the Kerr optical nonlinearity in Eq. (2) is expected to be weak. Neglecting the very small term containing n_j^2 in Eq. (1), we obtain the discontinuity of $dE(z)/dz$ for the jth optical scatterer at $z=z_j$ by integrating both sides of Eq. (1) in a very small region containing only $z=z_j$,

$$\frac{dE(z_j^+)}{dz}-\frac{dE(z_j^-)}{dz}=-\frac{2\omega^2}{c^2}n_b n_j E(z_j)=-2q^2\left(\frac{n_j}{n_b}\right)E(z_j), \tag{7}$$

where the notation z_j^+ (z_j^-) represents the right (left) side adjacent to the plane at $z=z_j$. Applying the boundary conditions to Eq. (6), i.e., $E(z)$ is continuous and $dE(z)/dz$ is discontinuous as described by Eq. (7), we find the following recurrence relation for the interface at $z=z_j$ with $1\leqslant j\leqslant N-1$:

$$\begin{bmatrix} f_j \\ b_j \end{bmatrix}=\begin{bmatrix} A_{11}^j & A_{12}^j \\ A_{21}^j & A_{22}^j \end{bmatrix}\begin{bmatrix} f_{j+1} \\ b_{j+1} \end{bmatrix}, \tag{8}$$

where the elements of the (2×2) coefficient matrix $\underline{\mathbf{A}}_j$ for the jth optical scatterer are

$$\begin{aligned} A_{11}^j&=[1-iq(n_j/n_b)]e^{-iqd_{j+1}}, \\ A_{12}^j&=-iq(n_j/n_b)e^{iqd_{j+1}}, \\ A_{21}^j&=iq(n_j/n_b)e^{-iqd_{j+1}}, \\ A_{22}^j&=[1+iq(n_j/n_b)]e^{iqd_{j+1}}, \end{aligned} \tag{9}$$

and $d_{j+1}=z_{j+1}-z_j$ is the separation between the $(j+1)$th and the jth optical scatterers. The left surface at $z=z_0=0$ provides us with an additional recurrence relation

$$\begin{bmatrix} s \\ \gamma \end{bmatrix}=\begin{bmatrix} A_{11}^0 & A_{12}^0 \\ A_{21}^0 & A_{22}^0 \end{bmatrix}\begin{bmatrix} f_1 \\ b_1 \end{bmatrix}, \tag{10}$$

where the elements of the (2×2) matrix coefficient $\underline{\mathbf{A}}_0$ for the first optical scatterer are

$$\begin{aligned} A_{11}^0&=[1-iq(n_0/n_b)]e^{-iqd_1}, \\ A_{12}^0&=-iq(n_0/n_b)e^{iqd_1}, \\ A_{21}^0&=iq(n_0/n_b)e^{-iqd_1}, \\ A_{22}^0&=[1+iq(n_0/n_b)]e^{iqd_1}, \end{aligned} \tag{11}$$

and $d_1=z_1-z_0\equiv z_1$ is the separation between the second and the first optical scatterers. In addition, the right surface at $z=z_N$ provides us with another recurrence relation

$$\begin{bmatrix} f_N \\ b_N \end{bmatrix}=\begin{bmatrix} A_{11}^N & A_{12}^N \\ A_{21}^N & A_{22}^N \end{bmatrix}\begin{bmatrix} t \\ 0 \end{bmatrix}, \tag{12}$$

where the elements of the (2×2) coefficient matrix $\underline{\mathbf{A}}_N$ for the last optical scatterer are

$$\begin{aligned} A_{11}^N&=[1-iq(n_N/n_b)]e^{iqz_N}, \\ A_{12}^N&=-iq(n_N/n_b)e^{-iqz_N}, \\ A_{21}^N&=iq(n_N/n_b)e^{iqz_N}, \\ A_{22}^N&=[1+iq(n_N/n_b)]e^{-iqz_N}. \end{aligned} \tag{13}$$

From the boundary conditions for $E(z)$, we know that it is continuous across any optical scatterers in the system. Therefore, according to Eqs. (3) and (6), we know that n_j depends only on f_{j+1} and b_{j+1}. This leads to the following expression for the nonlinear refractive index at each optical scatterer with $0\leqslant j\leqslant N$:

$$n_j=\begin{cases} (-1)^{j+1}\beta_K(|f_{j+1}e^{-iqd_{j+1}}+b_{j+1}e^{iqd_{j+1}}|^2) & \text{if } 0\leqslant j<N \\ (-1)^{N+1}\beta_K|t|^2 & \text{if } j=N, \end{cases} \tag{14}$$

where we note that $f_{j+1}e^{-iqd_{j+1}}+b_{j+1}e^{iqd_{j+1}}=f_j+b_j$ by the boundary condition, and therefore, there is no oscillation in n_j. Combining Eqs. (14) and (8), we are able to calculate the amplitude of the optical field at any position (labeled by indices $1\leqslant j\leqslant N$) using backward iterations within the disordered Fibonacci chain,

$$\begin{bmatrix} f_j \\ b_j \end{bmatrix} = \underline{\mathbf{A}}_j \otimes \underline{\mathbf{A}}_{j+1} \otimes \cdots \otimes \underline{\mathbf{A}}_{N-1} \otimes \underline{\mathbf{A}}_N \begin{bmatrix} t \\ 0 \end{bmatrix}, \quad (15)$$

where the notation $\otimes$ denotes the product of two matrices. Furthermore, combining Eqs. (14) and (15), we find the reflected (γ) and transmitted (t) field amplitudes for incident light as follows:

$$\gamma/s = M_{N+1}(2,1)/M_{N+1}(1,1),$$
$$t/s = 1/M_{N+1}(1,1), \quad (16)$$

where $M_{N+1}(2,1)$ and $M_{N+1}(1,1)$ are the two elements of the (2×2) matrix $\underline{\mathbf{M}}_{N+1}$ defined as[4]

$$\underline{\mathbf{M}}_{N+1} = \underline{\mathbf{A}}_0 \otimes \underline{\mathbf{A}}_1 \otimes \cdots \otimes \underline{\mathbf{A}}_{N-1} \otimes \underline{\mathbf{A}}_N. \quad (17)$$

For backward iterations, different values of s for incident field amplitude can be obtained by varying t in Eq. (16).

For a single planar optical scatterer, we get the following pair of equations:

$$q_0^2\beta_K^2|t|^6 + |t|^2 - |s|^2 = 0,$$
$$|t|^2 + |\gamma|^2 = |s|^2, \quad (18)$$

which is independent of n_b. From Eq. (18), we find $|t/s|^2 \to 1$ and $|\gamma/s|^2 \to 0$ for a transparent linear system when $|s|^2 \to 0$. On the other hand, when $|s|^2 \gg 1$, we get from Eq. (18) $|t/s|^2 \to (q_0\beta_K|s|^2)^{-2/3} \ll 1$ and $|\gamma/s|^2 \to 1-(q_0\beta_K|s|^2)^{-2/3} \approx 1$ for an opaque nonlinear system.

Based on the calculated field amplitudes γ and t for the reflected and transmitted optical waves in Eq. (16), we obtain the reflection coefficient R_{N+1} and the transmission coefficient T_{N+1} of the nonlinear disordered Fibonacci chain with $N+1$ optical scatterers as a function of the wave number q_0 and the field amplitude s of an incident light,

$$R_{N+1}(s,q_0) \equiv |\gamma/s|^2 = |M_{N+1}(2,1)/M_{N+1}(1,1)|^2,$$
$$T_{N+1}(s,q_0) \equiv |t/s|^2 = 1/|M_{N+1}(1,1)|^2. \quad (19)$$

By considering an incident light wave packet with a central wave number q_c and broadening σ_0, we calculate the average transmission coefficient over an interval $q_c-3\sigma_0 \leqslant q_0 \leqslant q_c+3\sigma_0$,

$$\bar{\mathcal{T}}(s,q_c,L) = \frac{1}{I_{max}+1}\sum_{i=0}^{I_{max}} T_{N+1}\left[s, q_c + \left(i - \frac{I_{max}}{2}\right)\Delta q\right], \quad (20)$$

where $I_{max}=6\sigma_0/\Delta q$ with $\Delta q/q_c=10^{-5}$ and $\sigma_0/q_c=10^{-2}$ in our numerical calculations below. The calculated $\bar{\mathcal{T}}(s,q_c,L)$ depends not only on how nonlinear-optical scatterers are distributed within a chain but also on the field amplitude s of the incident light. Furthermore, it changes with the chain length L or the total number of optical scatterers, where $L=(F_{n-2}a+F_{n-1}b)$ with $n \geqslant 2$ for the nth generation Fibonacci chain. The L dependence in $\bar{\mathcal{T}}(s,q_c,L)$ reflects the localization behavior.[19] The localization length $\xi_0(s,q_c)$ of a nonlinear disordered Fibonacci chain can be defined as[18,19]

$$\xi_0(s,q_c) = -\lim_{L\to\infty} \frac{L}{\ln[\bar{\mathcal{T}}(s,q_c,L)]}. \quad (21)$$

In addition, the dimensionless optical resistance for the disordered Fibonacci chain can be defined through the Landauer formula[13,19] by excluding the contact resistance

$$\bar{\mathcal{R}}_{op}(s,q_c,L) = 1 - \bar{\mathcal{T}}(s,q_c,L). \quad (22)$$

If the L-independent $\xi_0(s,q_c)$ becomes less than L when L is large, we say that a full localization has been reached in the system.[19] In this situation, $\bar{\mathcal{T}}(s,q_c,L)$ decreases exponentially with L.

III. NUMERICAL RESULTS AND DISCUSSIONS

Proposed layered nonlinear-optical scatterers embedded in a dielectric slab can be realized using nonlinear materials. Materials with β_K as high as 2×10^{-15} cm^3/V^2 are currently available.[31,32] With this value of β_K, the minimum laser power to switch a nonlinear device is about 4×10^5 W/cm^2. As a model calculation to demonstrate the interplay between optical nonlinearity and localization effect in a finite disordered Fibonacci chain, we set sample parameters $n_b=1.4$, $\beta_K=2\times 10^{-15}$ cm^3/V^2, $a=1000$ Å, and $b/a=\tau=(\sqrt{5}+1)/2$. The other parameters, such as N, p, and λ_0, will be given in the figure captions.

The interesting physics involved in this paper is the unique combination of optical nonlinearity and quasiperiodicity of the system. In a nonlinear-optical system described here, the transmission of an electromagnetic field depends on the amplitude of this incident wave as shown by Eq. (18), in strong contrast with a linear-optical system where the transmission is independent of the incident amplitude. The quasiperiodicity in the proposed nonlinear-optical system leads to localization effects, which makes the transmission of an electromagnetic field strongly depend on the length of the sample, in contrast with a periodic system where the transmission becomes independent of the sample length.

The construction of a disordered Fibonacci chain ($p=0.5$) is based on the random mix of a pure ($p=1$) and an inverted ($p=0$) Fibonacci chain. The randomness, in addition to the quasiperiodicity in a regular Fibonacci chain, leads to an enhanced localization effect in the disordered Fibonacci chain. Figure 2 displays the average transmission coefficients $\bar{\mathcal{T}}(s,q_c,L)$ defined in Eq. (20) [in (a)] and the dimensionless optical resistances $\bar{\mathcal{R}}_{op}(s,q_c,L)$ defined in Eq. (22) [in (b)] as functions of incident photon flux $|s|^2$ (in units of 10^8 V^2/cm^2) for nonlinear disordered (solid curves) and pure (dashed curves) Fibonacci chains with $N=F_9=55$ and $\lambda_0=6283$ Å. Randomness in the nonlinear disordered Fibonacci chain reduces $\bar{\mathcal{T}}(s,q_c,L)$ in (a) when $|s|^2$ or the optical-scattering strength ($n_j \propto \beta_K|s|^2$) of the system is moderate. However, this effect is suppressed when $|s|^2$ is small for a

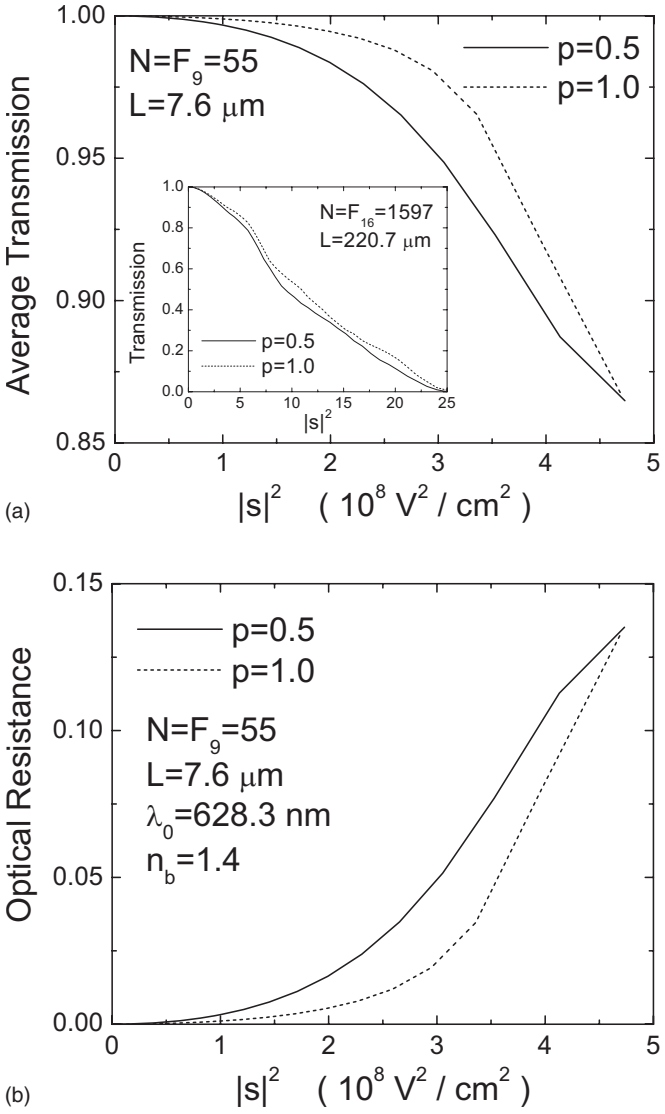

FIG. 2. Comparison of average transmission coefficients $\bar{\mathcal{T}}(s,q_c,L)$ [in (a)] and dimensionless optical resistances $\bar{\mathcal{R}}_{op}(s,q_c,L)$ [in (b)] as functions of incident photon flux $|s|^2$ in units of 10^8 V^2/cm^2 for nonlinear disordered ($p=0.5$, solid curves) and pure ($p=1$, dashed curves) Fibonacci chains with $N=F_9=55$ and $\lambda_0=6283$ Å. Here, the chain length $L=7.6$ μm. The inset in (a) shows the comparison of $\bar{\mathcal{T}}(s,q_c,L)$ for $p=0.5$ (solid curve) and $p=1$ (dashed curve) as functions of $|s|^2$ in units of 10^8 V^2/cm^2 with $N=F_{16}=1597$ and $L=220.7$ μm.

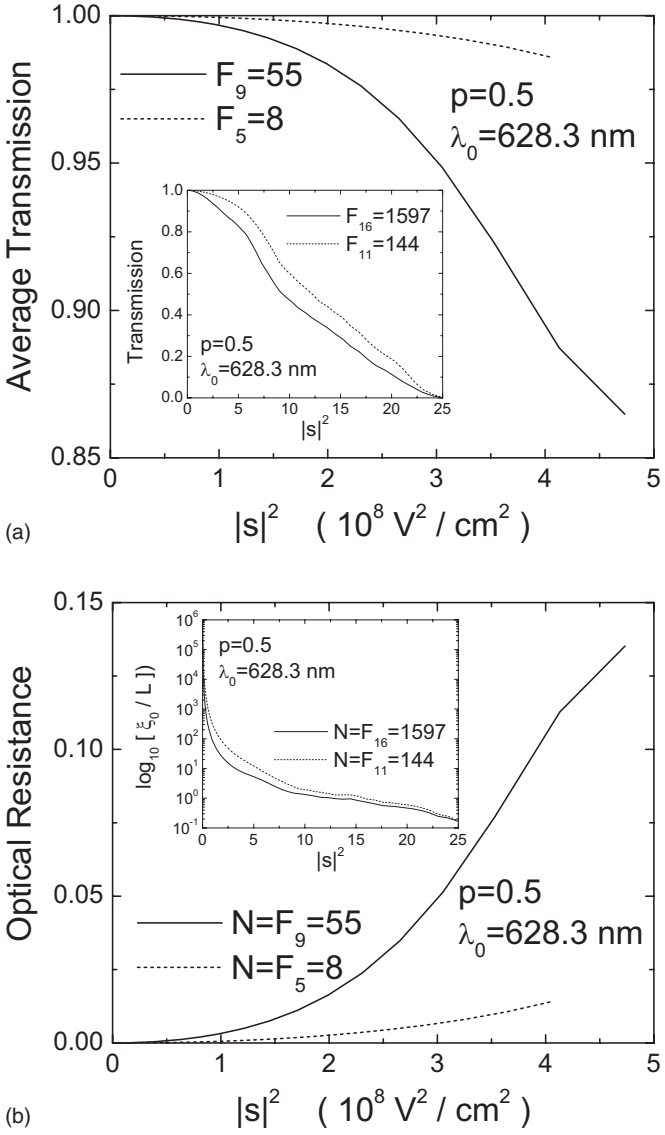

FIG. 3. Comparison of average transmission coefficients $\bar{\mathcal{T}}(s,q_c,L)$ [in (a)] and dimensionless optical resistances $\bar{\mathcal{R}}_{op}(s,q_c,L)$ [in (b)] as functions of incident photon flux $|s|^2$ in units of 10^8 V^2/cm^2 for $N=F_9=55$ (solid curves) an $N=F_5=8$ (dashed curves) in a nonlinear disordered Fibonacci chain with $p=0.5$ and $\lambda_0=6283$ Å. Here, the chain lengths L are 7.6 μm for $N=55$ and 1.1 μm for $N=8$, respectively. The inset in (a) shows the comparison of $\bar{\mathcal{T}}(s,q_c,L)$ for $N=F_{16}=1597$ (solid curve, $L=220.7$ μm) and $N=F_{11}=144$ (dashed curve, $L=19.9$ μm) as functions of $|s|^2$ in units of 10^8 V^2/cm^2 with $p=0.5$. The inset in (b) shows the comparison of $\log_{10}(\xi_0/L)$ for $N=F_{16}=1597$ (solid curve) and $N=F_{11}=144$ (dashed curve) as functions of $|s|^2$ in units of 10^8 V^2/cm^2 with $p=0.5$.

transparent linear-optical system. Moreover, when $|s|^2$ is large, the incident electromagnetic field tends to feel the dominant nonlinear-optical effect only from individual scatterers instead of the distribution of them. As a result, this makes the difference between $p=0.5$ and $p=1$ disappear in (a) when $|s|^2$ becomes high. We further find from (b) that the randomness in the disordered Fibonacci chain gradually enhances $\bar{\mathcal{R}}_{op}(s,q_c,L)$ when the optical nonlinearity ($\sim\beta_K|s|^2$) of the system initially increases from zero. From the inset of Fig. 2(a), we find that $\bar{\mathcal{T}}(s,q_c,L)$ almost drops to zero for large values of $|s|^2$ when the number of scatterers is increased to $N=F_{16}=1597$, where $\xi_0/L\sim 0.2$ indicating a strong localization effect.

The localization effect in a disordered Fibonacci chain also increases with the number N of optical scatterers in the system or the chain length $L=(F_{n-2}a+F_{n-1}b)$. In Fig. 3, we compare $\bar{\mathcal{T}}(s,q_c,L)$ [in (a)] and $\bar{\mathcal{R}}_{op}(s,q_c,L)$ [in (b)] as functions of $|s|^2$ for nonlinear disordered Fibonacci chains with

$N=F_9=55$ (solid curves) and with $N=F_5=8$ (dashed curves) at $\lambda_0=6283$ Å. From (a), we find that the optical nonlinearity slightly decreases $\bar{\mathcal{T}}(s,q_c,L)$ when the chain is short ($L \sim \lambda_0$), where only a few nonlinear-optical scatterers ($N=8$) exist in the system. On the other hand, $\bar{\mathcal{T}}(s,q_c,L)$ decreases greatly with $|s|^2$ when the chain is long ($L \sim 10\lambda_0$), where there are a lot of scatterers ($N=55$) in the system. Correspondingly, $\bar{\mathcal{R}}_{op}(s,q_c,L)$ in (b) is seen to increase with $|s|^2$ dramatically when the chain is long and the number of nonlinear-optical scatterers in the system is large. From this, we know that the localization effect of the system is able to enhance the nonlinear-optical scattering in the chain. From the inset of Fig. 3(a), we can clearly see that the difference in $\bar{\mathcal{T}}(s,q_c,L)$ for large values of $|s|^2$ is greatly enhanced when the number of scatterers increases from $N=F_{11}=144$ to $N=F_{16}=1597$. In order to quantify the effect of localization in the chain, we numerically calculate ξ_0/L in Eq. (21) and display it for disordered Fibonacci chains as a function of $|s|^2$ in the inset of Fig. 3(b) with $N=F_{16}=1597$ (solid curve) and $N=F_{11}=144$ (dashed curve) at $\lambda_0=6283$ Å. From this inset, we find that ξ_0/L dramatically decreases with $|s|^2$ by more than 6 orders of magnitude from a transparent ($\xi_0/L \to \infty$) to a nearly opaque ($\xi_0/L \to 0$) optical system. When the chain length is increased from $L=19.9$ μm ($N=F_{11}=144$) to $L=220.7$ μm ($N=F_{16}=1597$), ξ_0/L decreases nearly by an order of magnitude with moderate $|s|^2$, indicating a strong localization effect from randomness in a disordered Fibonacci chain. When ξ_0/L drops below unity, the full localization of the system with $\xi_0/L \propto 1/L$ has been reached for $N=F_{16}=1597$. Moreover, ξ_0/L becomes independent of N when $|s|^2$ is very small. If $|s|^2 \to 0$, ξ_0/L tends to infinity, corresponding to a transparent dielectric slab in the absence of embedded optical scatterers since $n_j \propto \beta_K |s|^2$. Consequently, a large optical nonlinearity of the system for intense light illumination can be employed for speeding up the localization effect in the chain when enough nonlinear-optical scatterers are present.

The more energetic the incident photons are, the less the effective number of embedded optical scatterers is seen by them while flying through a chain. This effect can be clearly seen from Fig. 4, where we plot $\bar{\mathcal{T}}(s,q_c,L)$ [in (a)] and $\bar{\mathcal{R}}_{op}(s,q_c,L)$ [in (b)] as functions of $|s|^2$ in a nonlinear disordered Fibonacci chain with $N=F_9=55$ for $\lambda_0=6283$ Å (solid curves) and $\lambda_0=4833$ Å (dashed curves). When $|s|^2$ is large, a smaller photon energy (solid curve with a larger λ_0) leads to a significant reduction of $\bar{\mathcal{T}}(s,q_c,L)$ in (a) due to the presence of many nonlinear-optical scatterers in the system. On the other hand, photons tend to ignore most of the deep optical scatterers in the system when their energy is large. In this case, $\bar{\mathcal{T}}(s,q_c,L)$ becomes less sensitive to $|s|^2$, as explained in Fig. 3(a) for very few optical scatterers. When $|s|^2$ is large, the dependence of $\bar{\mathcal{T}}(s,q_c,L)$ on q_c causes $\bar{\mathcal{R}}_{op}(s,q_c,L)$ to exhibit an enhancement in (b) with a smaller photon energy. The above explanation also holds for a much longer chain (not shown here).

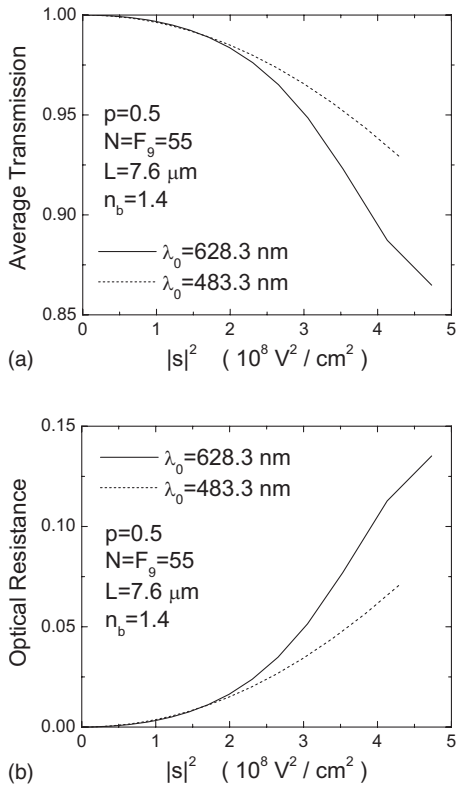

FIG. 4. Comparison of average transmission coefficients $\bar{\mathcal{T}}(s,q_c,L)$ [in (a)] and dimensionless optical resistances $\bar{\mathcal{R}}_{op}(s,q_c,L)$ [in (b)] as functions of incident photon flux $|s|^2$ in units of 10^8 V^2/cm^2 for $\lambda_0=6282$ Å (solid curves) and $\lambda_0=4833$ Å (dashed curves) in a nonlinear disordered Fibonacci chain with $p=0.5$ and $N=F_9=55$. Here, the chain length $L=7.6$ μm.

IV. CONCLUSION

We have calculated in this paper the average transmission coefficients and dimensionless optical resistances as functions of the square of the incident field amplitude for different types of chains of scatterers, numbers of embedded nonlinear-optical scatterers, and energies of incident photons. When the incident photon flux is very low, the nonlinear-optical scattering can be neglected and the system behaves just like a transparent dielectric slab. We have concluded as follows for the interplay between the optical nonlinearity and localization effect in a finite disordered Fibonacci chain: (1) the localization effect in a disordered Fibonacci chain can play a significant role only when the incident light field is strong; (2) the localization effect, which increases with the number of optical scatterers, can lead to an enhancement of the nonlinear-optical scattering in a chain; (3) a large optical nonlinearity with an intense light illumination can speed up the localization effect in a chain in the presence of many nonlinear-optical scatterers; and (4) energetic photons tend to ignore most of the deep nonlinear-optical scatterers embedded in a chain. In addition, when $N=F_{16}=1597$, a full localization in the chain has been reached for $s=50$ kV/cm.

As a final remark, the use of nonlinear-optical scatterers with the strength $n_j \propto \beta_K |s|^2$ embedded in an refractive-index-matched chain ensures that the chain behaves just like a

transparent dielectric slab when the intensity of the incident light field is weak. On the other hand, when the incident light intensity exceeds a threshold value, the strong optical scattering will greatly reduce the light transmission due to quasiperiodically distributed nonlinear scatterers inside the chain. In addition, the randomness introduced in the disordered Fibonacci chain further speeds up the localization effect on the incident optical wave to make its transmission exponentially small when the chain is long and the incident light is intense.

ACKNOWLEDGMENTS

D.H. would like to thank the AFOSR for support.

*Also at La Cueva High School, 7801 Wilshire Blvd. NE, Albuquerque, NM 87122.
†Corresponding author. Electronic address: danhong.huang@kirtland.af.mil

[1] T. Apostolova, D. H. Huang, P. M. Alsing, J. McIver, and D. A. Cardimona, Phys. Rev. B **66**, 075208 (2002).
[2] T. Apostolova, D. H. Huang, and D. A. Cardimona, Phys. Rev. B **67**, 205323 (2003).
[3] D. H. Huang, P. M. Alsing, T. Apostolova, and D. A. Cardimona, Phys. Rev. B **71**, 045204 (2005).
[4] Y. Zhao, D. H. Huang, and R. Shen, J. Nonlinear Opt. Phys. Mater. **4**, 1 (1995).
[5] E. Yablonovitch, Phys. Rev. Lett. **58**, 2059 (1987); E. Yablonovitch and T. J. Gmitter, *ibid.* **63**, 1950 (1989).
[6] E. Yablonovitch, T. J. Gmitter, and K. M. Leung, Phys. Rev. Lett. **67**, 2295 (1991); E. Yablonovitch, T. J. Gmitter, R. D. Meade, A. M. Rappe, K. D. Brommer, and J. D. Joannopoulos, *ibid.* **67**, 3380 (1991).
[7] K. M. Ho, C. T. Chan, and C. M. Soukoulis, Phys. Rev. Lett. **65**, 3152 (1990).
[8] M. Plihal, A. Shambrook, A. A. Maradudin, and P. Sheng, Opt. Commun. **80**, 199 (1991); S. L. McCall, P. M. Platzman, R. Dalichaouch, D. Smith, and S. Schultz, Phys. Rev. Lett. **67**, 2017 (1991).
[9] J. Martorell and N. M. Lawandy, Phys. Rev. Lett. **65**, 1877 (1990).
[10] P. W. Anderson, Phys. Rev. **109**, 1492 (1958).
[11] D. H. Huang, Phys. Rev. B **53**, 13645 (1996).
[12] L. Esaki, IEEE J. Quantum Electron. **QE-22**, 1611 (1986).
[13] R. Landauer, IBM J. Res. Dev. **1**, 223 (1957); D. S. Fisher and P. A. Lee, Phys. Rev. B **23**, 6851 (1981).
[14] D. Shechtman, I. Blech, D. Gratias, and J. W. Cahn, Phys. Rev. Lett. **53**, 1951 (1984).
[15] Y. Avishai and D. Berend, Phys. Rev. B **41**, 5492 (1990); M. Kolář and M. K. Ali, *ibid.* **39**, 426 (1989); M. Kohmoto, L. P. Kadanoff, and C. Tang, Phys. Rev. Lett. **50**, 1870 (1983); Q. Niu and F. Nori, *ibid.* **57**, 2057 (1986); Z. Cheng, R. Savit, and R. Merlin, Phys. Rev. B **37**, 4375 (1988).
[16] B. Simon, Adv. Appl. Math. **3**, 463 (1982); J. B. Sokoloff, Phys. Rep. **126**, 189 (1985).
[17] D. H. Huang, J. P. Peng, and S. X. Zhou, Phys. Rev. B **40**, 7754 (1989).
[18] D. H. Huang, G. Gumbs, and M. Kolăr, Phys. Rev. B **46**, 11479 (1992).
[19] D. H. Huang and D. R. Huang, Phys. Rev. B **70**, 205124 (2004).
[20] D. H. Huang and G. Gumbs, Solid State Commun. **84**, 1061 (1992).
[21] G. Gumbs, G. S. Dubey, A. Salman, B. S. Mahmoud, and D. Huang, Phys. Rev. B **52**, 210 (1995).
[22] D. H. Huang, G. Gumbs, Y. Zhao, and G. W. Auner, Phys. Lett. A **200**, 459 (1995).
[23] D. H. Huang, A. Singh, and D. A. Cardimona, Phys. Lett. A **259**, 488 (1999).
[24] D. H. Huang, D. A. Cardimona, and A. Singh, Phys. Lett. A **243**, 335 (1998).
[25] H. Furstenberg, Trans. Am. Math. Soc. **108**, 377 (1963).
[26] D. Viswanath, Math. Comput. **69**, 1131 (2000).
[27] J. C. López, G. Naumis, and J. L. Aragón, Phys. Rev. B **48**, 12459 (1993).
[28] C. Sire and P. L. Krapivsky, J. Phys. A **34**, 9065 (2001).
[29] J. C. López, G. Naumis, and J. L. Aragón, Phys. Rev. B **48**, 12459 (1993).
[30] V. M. Agranovich, S. A. Kiselev, and D. L. Mills, Phys. Rev. B **44**, 10917 (1991).
[31] K. M. Yoo and R. R. Alfano, Opt. Lett. **16**, 1823 (1991).
[32] C. J. Herbert, W. S. Capinski, and M. S. Malcuit, Opt. Lett. **17**, 1037 (1992).